White Matter Microstructure and Structural Networks in Treatment-Resistant Schizophrenia Patients After Commencing Clozapine Treatment: A Longitudinal Diffusion Imaging Study

Authors

Giulia Tronchin[1], Genevieve McPhilemy[1], Mohamed Ahmed[1], Liam Kilmartin[2], Laura Costello[1], Natalie J. Forde[3], Leila Nabulsi[1,4], Theophilus N. Akudjedu[1,5], Laurena Holleran[1], Brian Hallahan[1], Dara M. Cannon[1] and Colm McDonald[1]

Affiliations:

[1]*Centre for Neuroimaging & Cognitive Genomics (NICOG), Clinical Neuroimaging Laboratory, NCBES Galway Neuroscience Centre, College of Medicine Nursing and Health Sciences, National University of Ireland Galway, H91TK33 Galway, Ireland.*

[2]*College of Science and Engineering, National University of Ireland Galway, Galway, Republic of Ireland*

[3]*Radboud University Medical Centre, Donders Institute for Brain, Cognition and Behaviour, Nijmegen, Netherlands*

[4]*Imaging Genetics Center, Mark and Mary Stevens Neuroimaging & Informatics Institute, University of Southern California, Marina del Rey, CA 90292, USA*

[5]*Institute of Medical Imaging & Visualisation, Faculty of Health & Social Science, Bournemouth University, Bournemouth, United Kingdom.*

Abstract

Clozapine has a superior clinical effect in refractory schizophrenia, however its potential impact on white matter microstructure and neural networks is unclear. This study investigates such changes after 6 months of switching to clozapine in schizophrenia patients compared to controls, and whether any changes are related to clinical variables.

T1 and diffusion-weighted MRI images were acquired at baseline before commencing clozapine and after 6 months of treatment for 22 patients with treatment-resistant schizophrenia and 23 controls. The Tract-based spatial statistics approach was used to compare changes over time between groups in fractional anisotropy (FA). Changes in structural network organisation and subnetwork connectivity weighted by FA and number of streamlines were assessed using graph theory and network-based statistics.

Patients displayed a significant reduction of FA over time ($p<0.05$) compared to controls in the genu and body of the corpus callosum and bilaterally in the anterior and superior corona radiata. There was no correlation between FA change in patients and changes in clinical variables or serum level of clozapine. There was no significant overall interaction between time, group and structural network global ($F_{(7,280)}= 2.80; p=0.187$) or local ($F_{(15,600)}= 0.747$, $p=0.737$) measures. No subnetwork was identified when testing for time by group interaction.

This longitudinal study demonstrated progressive focal FA abnormalities in key anterior tracts, such as corpus callosum and corona radiata, but preserved brain structural network organisation in patients. The FA reduction was independent of any clinical measures and may reflect progression of the underlying pathophysiology of this malignant form of schizophrenia illness.

1. Introduction

Schizophrenia is a complex and heterogenous mental illness, defined as conduction deficit by Eugen Bleuler during the 20th century (Bleuler, 1911), and nowadays through the development of advanced neuroimaging techniques is conceived as a dysconnectivity disorder characterized by disturbed integration of functions between different brain areas (Friston and Frith, 1995). Diffusion Magnetic Resonance imaging (dMRI), which provides an indirect measure of the microstructural organization of white matter (WM) (Jones, 2008), has found evidence of white matter dysconnectivity in schizophrenia. Fractional anisotropy (FA), the most reported dMRI outcome measure, reflects the heterogeneous water diffusion in WM, which is sensitive to fibre orientation, coherence, density and degree of myelination of neurons within fibre bundles (Beaulieu, 2002; Pierpaoli et al., 1996; Tournier et al., 2011).

dMRI meta-analyses have reported significant FA reductions in schizophrenia patients compared to controls in WM tracts interconnecting the frontal lobe, thalamus, cingulate and tracts traversing left temporal WM regions (Bora et al., 2011; Ellison-wright and Bullmore, 2009). A large-scale international collaborative metanalysis (ENIGMA) based on 2359 healthy controls and 1963 schizophrenia patients reported significant widespread FA reductions in schizophrenia patients, most prominent in the anterior corona radiata and the body and genu of the corpus callosum (Kelly et al., 2017). Another recent meta-analysis by Vitolo and colleagues (2017) of voxel-based morphometry and diffusion tensor imaging (DTI) studies focusing on WM alterations between schizophrenia patients and controls, based on 59 studies, reported widespread alteration of white matter bundles, including frontal, temporal, and limbic pathways. Other circuits such as callosal, commissural, and cortico-cerebellar-thalamic-cortical were also altered in schizophrenia patients compared to controls (Vitolo et al., 2017).

Although treatment resistance, usually defined as failure to respond to at least two adequate trials of classic antipsychotic medications (Suzuki et al., 2012), affects approximately 30% of patients with schizophrenia (Lieberman et al., 1994; Meltzer, 1997), few diffusion weighted studies have specifically investigated this illness subtype. Cross-sectional voxel based-morphometry studies of treatment-resistant schizophrenia patients (TRS) have reported decreased whole brain white matter compared with controls (Anderson

et al., 2015; Maller et al., 2012). In contrast, Molina et al., (Molina et al., 2008) found significant white matter volume increase in the frontal, parietal and occipital lobe in treatment-resistant patients compared to controls. Previously, a case control DTI study from our group examining white matter volume in chronic severe treatment resistant schizophrenia, who had not yet commenced clozapine treatment, reported reduced FA with corresponding increased radial diffusivity in the genu, body, and splenium of the corpus callosum, the right posterior limb of the internal capsule, right external capsule, and the right temporal inferior longitudinal fasciculus in patients compared to controls (Holleran et al., 2013).

However, none of these cross-sectional studies were able to assess whether introducing clozapine treatment may affect measures of structural connectivity in schizophrenia. Clozapine has an established superior clinical effect in refractory schizophrenia, with 60-70% of patients showing a positive response (Chakos et al., 2001; Kane et al., 1988; Stroup et al., 2003), however, its effect on brain structures and neural networks is still unclear. In previous works from our group, we demonstrated on-going cortical thinning of the left medial frontal cortex, right middle temporal cortex and a progressive subcortical volumetric reduction in patients with treatment-resistant schizophrenia after 6 months of switching to clozapine treatment (Ahmed et al., 2015; Tronchin et al., 2020a), despite symptomatic improvement. Molina et al., in a small 6-month longitudinal volumetric study of T1 weighted images found that 13 TRS patients who had started clozapine treatment presented a marked decrease in frontal, parietal and occipital white matter compared to 11 controls (Molina et al., 2008). In contrast, a longitudinal DTI study by Ozcelik-Eroglu et al., (2014) based on 16 schizophrenia patients and 8 controls and investigating the effect of 12 weeks of clozapine treatment on white matter, reported in the patient group increased FA values in 31 regions at follow-up compared to baseline. When comparing these changes with the control group the study reported significant FA increases in patients in the left superior parietal lobule and the left inferior fronto-occipital fasciculus (Ozcelik-Eroglu et al., 2014).

Structural Networks

In recent years focus has shifted to study the entire structural connectivity of the brain, through network analysis, which has offered a complementary approach to explore the concept of dysconnectivity (Fornito et al., 2015, 2012, Sporns, 2013a, 2013b). Employing

graph theory, structural networks can be modelled using metrics derived from structural magnetic resonance imaging and dMRI, where cortical and subcortical structures are defined as "nodes" and white matter connections as "edges" (Bullmore and Sporns, 2009). When nodes and edges are mapped, the brain, conceived as a graph, can be assessed for its topological properties, such as efficiency and pattern of connections. Such techniques enable the investigation of connectivity features that are not otherwise measurable by focusing on information from single brain regions (Van Den Heuvel and Fornito, 2014).

Network studies have reported impaired structural connectivity in schizophrenia (Fornito et al., 2012; Pettersson-Yeo et al., 2011), including reductions in global communication efficiency (Zalesky et al., 2011) and related longer average path length (Ottet et al., 2012; Van Den Heuvel et al., 2010; Zhang et al., 2012). In particular, Van den Heuvel and colleagues, in a cross-sectional study based on 40 schizophrenia patients and 40 healthy controls reported reduced global efficiency of the frontal, temporal, and occipital brain regions in schizophrenia (Van de heuvel 2010). A recent cross sectional study (Luo et al., 2020) explored the characteristics of structural network in chronic schizophrenia patients (never treated n=17, treated with clozapine (n=17) and risperidone (n=17) monotherapy for over 5 years). The study suggested a general disruption in the organization of white matter structural networks as well as decreased nodal and connectivity characteristics across all the schizophrenia groups, specifically the alteration was more prominent in never treated and clozapine treated patients. Kraguljac and colleagues (Kraguljac et al., 2019) investigated in 42 patients with schizophrenia, who were medication naïve or off antipsychotic medications for at least 2 weeks, the effect of a trial of risperidone on white matter diffusion indices. The study observed no changes in micro- or macrostructural white matter after 6 weeks of treatment in patients with schizophrenia.

Recently, Mackay and colleagues (2018) (Mackay et al., 2018), published a review analysing current findings of system-level brain dysconnectivity in treatment-resistant schizophrenia patients, suggesting that this group compared to chronic schizophrenia present unique biological circuitry, characterized by a pronounced and widespread dysfunction throughout the entire brain, involving both cortical and subcortical regions. A cross-sectional functional network-based study reported widespread reductions in functional connectivity at the whole brain level in treatment-resistant schizophrenia patients compared to controls, specifically involving temporal, occipital and frontal regions. They also reported reduced global efficiency

and increased local efficiency in patients compared to controls (Ganella et al., 2017). To our knowledge, there are no studies investigating structural network changes longitudinally in treatment-resistant schizophrenia patients exposed to clozapine treatment.

The present study sought to comprehensively investigate whether, after 6 months of switching to clozapine, white matter microstructure and structural network organisation demonstrate any progressive changes in a unique sample of treatment-resistant clozapine-naïve schizophrenia patients compared to healthy controls. We also sought to assess whether any connectivity changes were related to clinical variables and serum level of clozapine at follow-up.

2. Method

2.1 Participants

As previously reported (Ahmed et al., 2015; Tronchin et al., 2020a) 33 patients with treatment-resistant schizophrenia (TRS) and 31 healthy volunteers (HC) matched for sex and age successfully participated at both baseline, prior to clozapine initiation in patients, and 6 months follow-up clinical assessments and MRI scanning. Of these 64 participants, diffusion MRI data were available at both time points for 22 patients and 23 healthy controls (Table 1). Patients and controls were excluded from the study if they had a history of a previous trial of clozapine treatment, a learning disability, history of neurological illness, history of head injury which resulted in loss of consciousness for over 5 minutes, use of oral steroids in the three months prior to participation, history of comorbid alcohol/ substance dependency as defined by the DSM-IV or any contraindication to MRI scanning. Exclusion criteria for controls also included having a current or past axis I disorder (DSM-IV-TR) or any psychotic disorder in a first-degree relative. The study was approved by the Galway University Hospital Clinical Research Ethics Committee. Fully informed written consent was obtained for all participants.

2.2 Clinical assessment

All patients were diagnosed using the Diagnostic and Statistical Manual for Mental Disorders 4th Edition text revision (DSM-IV-TR) (American Psychiatric Association, 2000). Treatment resistance was defined as the failure to respond to at least two adequate trials of antipsychotic medications (normally 6 months), including at least one atypical antipsychotic drug, with a prolonged period of moderate to severe positive and/or negative symptoms (National Institute of Health and Clinical Excellence, 2014). The severity of positive and negative symptoms was assessed at both time points using the Positive and Negative Syndrome Scale (PANSS) (Kay et al., 1987), The Scale for the Assessment of Positive Symptoms (SAPS) (Andreasen, 1982a) and The Scale for the Assessment of Negative Symptoms (SANS) (Andreasen, 1982b). Social, occupational and psychological functioning was assessed using a Global Assessment Functioning Score (Hall, 1995). As previously described (Tronchin et al., 2020a) we used the symptomatic remission criteria of Andreasen et al., (Andreasen et al., 2005) with the exclusion of the maintenance over 6-month observation period (Egerton et al., 2018) in order to categorically determine treatment response.

2.3 *MRI data acquisition*

MRI images were acquired for all participants at baseline and after 6 months at University Hospital Galway in a 1.5 Tesla Siemens Magnetom Symphony scanner (Erlangen, Germany) equipped with a 4-channel head coil. Magnetisation prepared rapid gradient-echo (MPRAGE) sequence was employed to acquired high resolution volumetric T1-weighted images, with the following parameters: repetition time (TR): 1140 ms, echo time (TE): 4.38 ms, inversion time (TI): 600 ms, flip angle: 15°, matrix size: 256x256, interpolated to 512 x 512, slice thickness: 0.9 mm and in plane resolution: 0.45 mm x 0.45 mm. Diffusion-weighted MRI data were collected with a standard 8-channel head coil using an echo planar imaging (EPI) diffusion sequence acquired with parallel imaging. The acquisition parameters were as follows; 64 independent diffusion gradient directions, comprising 2 separate multi-direction diffusion-weighted sequences that are subsequently concatenated in ExploreDTI (Leemans et al., 2009), including 7 reference images with no diffusion gradient (B_0) i.e. (34 directions + $3B_0$) & (37 directions +$4B_0$), *b* = 1300s/m. m^2, TR = 8100ms, TE = 95ms, FOV = 240 x 240mm^2, matrix size 96 x 96, 60 axial slices and total imaging time of 10.24 minutes generating an in plane resolution of 2.5mm x 2.5mm with slice thickness of 2.5 mm.

2.4 MRI processing

T1-weighted images were processed through the longitudinal stream (Reuter et al., 2012) of Freesurfer v.5.3.0 ("FreeSurfer," 2013) to parcellate cortical and subcortical regions at two time points. The several steps of the processing pipeline to obtain the output have previously been described in detail (Tronchin et al., 2020b). At each step, the output was visually inspected, to verify that the parcellation was anatomically accurate and computationally successful ("FreeSurfer Quality Control Guide," 2013). At each time point, diffusion-weighted images were corrected for motion artefacts, eddy -current distortions and rotation of the b-matrix using ExploreDTI v4.8.6. The data quality was defined after visually inspecting for geometric distortion, subject head motion, signal dropout, abnormal model residuals and registration accuracy (Tournier et al., 2011). Following quality check, no images were excluded.

2.5 Voxel-based Statistical Analysis and Statistic

Voxel-by-voxel based statistical analysis was performed using the tract-based spatial statistic (TBSS) approach (Smith and Nichols, 2009) for baseline analysis and adapted for longitudinal analysis ("FSL Support"). The Fractional Anisotropy images were exported from the diffusion motion corrected native images, using ExploreDTI v4.8.6 (Leemans et al., 2009). Subject-specific registration was employed, all FA images were non-linearly aligned to the target subject specific image and subsequently the affine transformation to standard MNI152 1mm^3 space was applied (FSL v. 6.0.1). All the individual FA images were merged and averaged to get a mean FA image. Then, a study-specific thinned mean FA skeleton was produced (0.2 FA threshold was applied to exclude non-WM voxels). Each individual subject's FA image was projected onto the skeleton by searching perpendicular to the skeleton to find the maximum FA for use in the statistical analysis. At each of the previous steps a qualitative analysis was carried out. Only for the longitudinal analysis FA difference maps were then produced for each subject (Baseline – Follow-up) (De Groot et al., 2016; Minett et al., 2018; Reis Marques et al., 2014). Randomise voxel-wise statistics analysis was performed and threshold-free cluster enhancement (TFCE) applied to correct for multiple comparisons ($p<0.05$)(Nichols and Holmes, 2003; Smith and Nichols, 2009). Age and sex were included as covariates in the model. The John Hopkins University (JHU) ICBM_DTI_81 white-matter labels atlas (Wakana et al., 2007) was used to identify clusters that showed significant statistical group differences. Significant clusters were masked and FA at baseline and FA change over time was extracted ("fslwiki Cluster," 2013). For the patient group FA at baseline and FA change over time was correlated with change in clinical and anthropomorphic variables and serum level of clozapine at follow-up using Partial correlation covarying for age and sex and Spearman correlation where appropriate (SPSS v23). To estimate longitudinally the values of other white matter difusion tensor imaging parameters, such as mean diffusivity (MD) (The level of water diffusion in any direction at each point of the tract, which increases with loss of structural barriers that normally restrict water diffusion) and radial diffusivity (RD) (The degree of diffusion perpendicular to the primary tract axis; where a marked increase may be associated with demyelination) (Song et al., 2003, 2002; Van Den Heuvel and Fornito, 2014), the original FA nonlinear registration was applied to the non-FA data, and subsequently projected into the original mean FA skeleton. Randomise voxel-wise statistical analysis was performed as

described above. An additional one-way MANCOVA was performed to assess differences between clozapine responders and non-responders at baseline on FA at baseline, covarying for age and sex. A visual description of this pipeline is outlined in Figure 1.

Voxel-based Statistical Analysis and Statistic
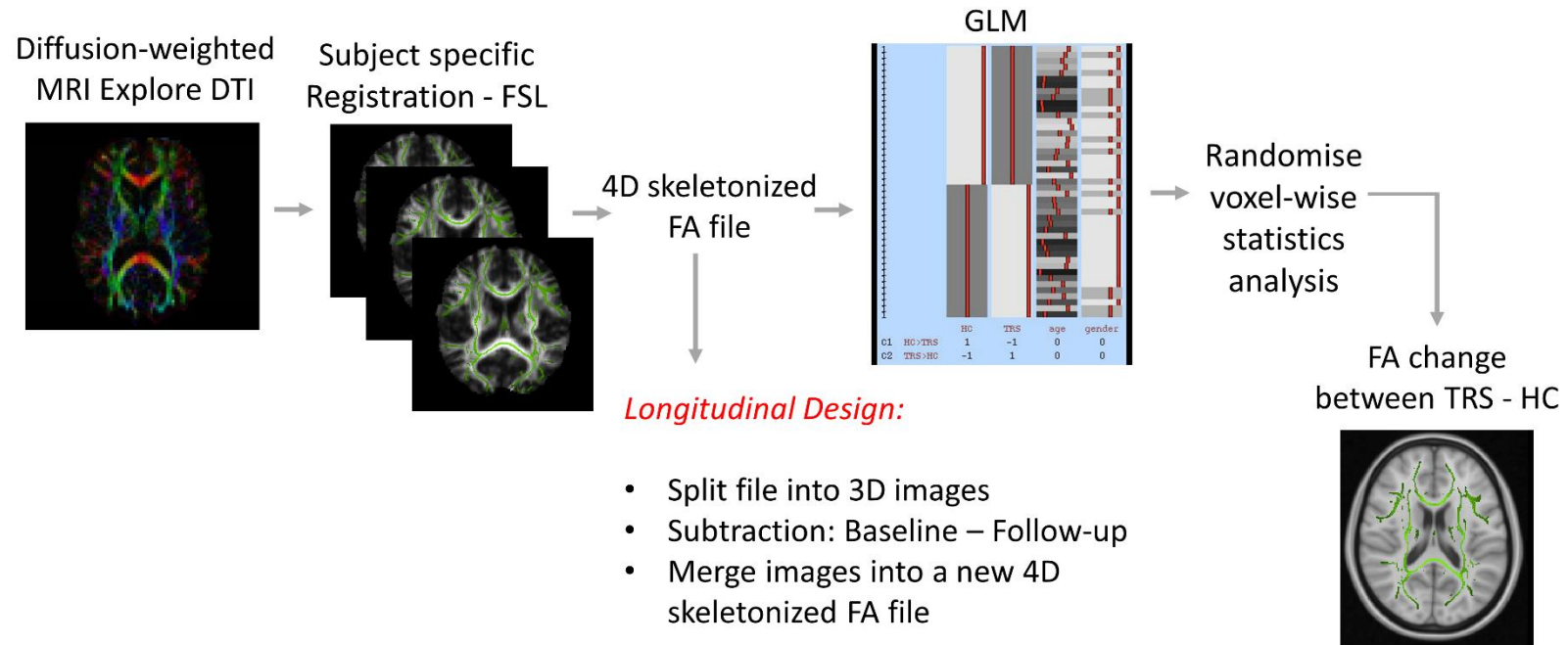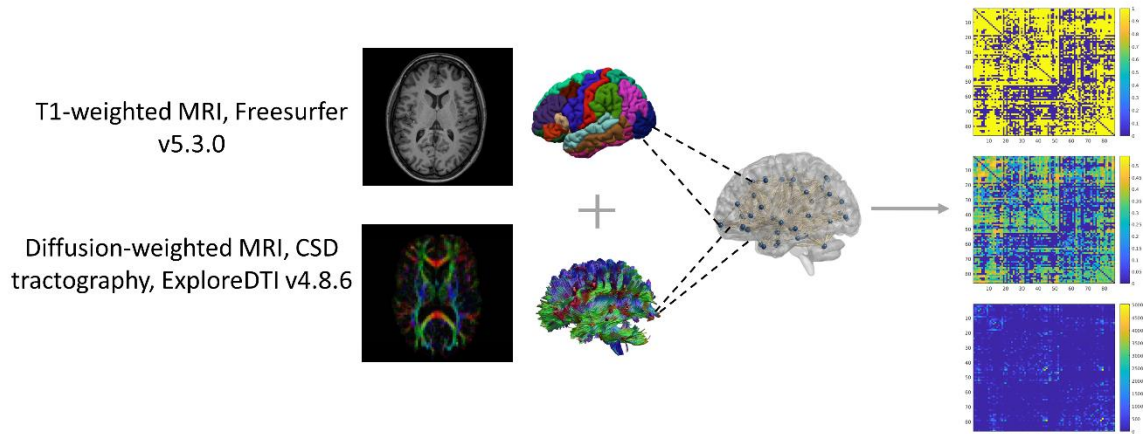Tract-based spatial statistic (TBSS) approach

Figure 1. Voxel-based Statistical Analysis Method

2.6 Network Reconstruction and Statistic

A deterministic non-tensor-based constrained spherical deconvolution (CSD) algorithm was applied to the motion corrected diffusion-weighted data and included recursive calibration of the response function (ExploreDTI v4.8.6) (Jeurissen et al. 2011; Tournier et al. 2008). Fiber tracking commenced in each voxel, continued with 1 mm step size, 2 mm^3 seed point resolution, and terminated at >30° angle curvature, <20 or >300 mm in length, and <0.2 FA. Eighty-six regions, including 34 cortical, 8 subcortical and cerebellar hemispheres bilaterally were defined using the longitudinal pipeline of Freesurfer v5.3.0, based on the Desikan-Killiany atlas (Desikan et al., 2006; Fischl., 2002). For each participant and at each time point, unweighted connectivity matrices (86x86) were generated (ExploreDTI v4.8.6) and connections that were present in each subject at both baseline and follow-up were retained to increase sensitivity in changes over time. The identified connections were used as definition of which weights to keep at baseline and follow-up for matrices weighted by fractional anisotropy (FA) and number of reconstructed streamlines (NOS). Quality check involved ensuring that post-thresholded networks remained fully connected which resulted in the removal of 1 healthy control. Global measures of whole-brain connectivity including global efficiency, characteristic path length, average clustering coefficient and average strength were derived from weighted matrices. Local measures of clustering coefficient and strength were obtained from weighted matrices (Brain Connectivity Toolbox v1.52)(Rubinov and Sporns, 2010) for thalamus, putamen, caudate and hippocampus, whose volume was found decreased over time in patients compared to controls in our previous work (Tronchin et al., 2020a). An initial one-way multivariate analysis of covariance (MANCOVA) was performed to evaluate differences between groups at baseline on global and subsequently local network measures, covarying for age and sex. Thereafter two-way repeated MANCOVA was used to assess the course of changes in global and local network measures over time between patients and controls, covarying for age and sex. An additional one-way MANCOVA was performed to assess differences between clozapine responders and non-responders at baseline on subcortical structures, covarying for age, sex. A visual description of this methodological pipeline is outlined in Figure 2.

Structural Connectivity

A

T1-weighted MRI, Freesurfer v5.3.0

Diffusion-weighted MRI, CSD tractography, ExploreDTI v4.8.6

B

Longitudinal Design

i

Baseline - Unweighted   Follow-up - Unweighted

Mask - Binary

ii

Matrices weighted by Fractional Anisotropy (FA)   Matrices weighted by Number of Streamlines (NOS)

iii

Global measures	Local measures	Subnetwork measures
Two-way repeated ANCOVA	Two-way repeated ANCOVA	**nbs** CONNECTOME

- Global Efficiency
- Characteristic Path Length
- Clustering Coefficient
- Strength

- Clustering Coefficient
- Strength

iv Subtraction Matrices: Baseline – Follow Up

Fractional Anisotropy (FA)   Number of Streamlines (NOS)

Statistic:
- F-statistic threshold of 1.75, 2, 2.5
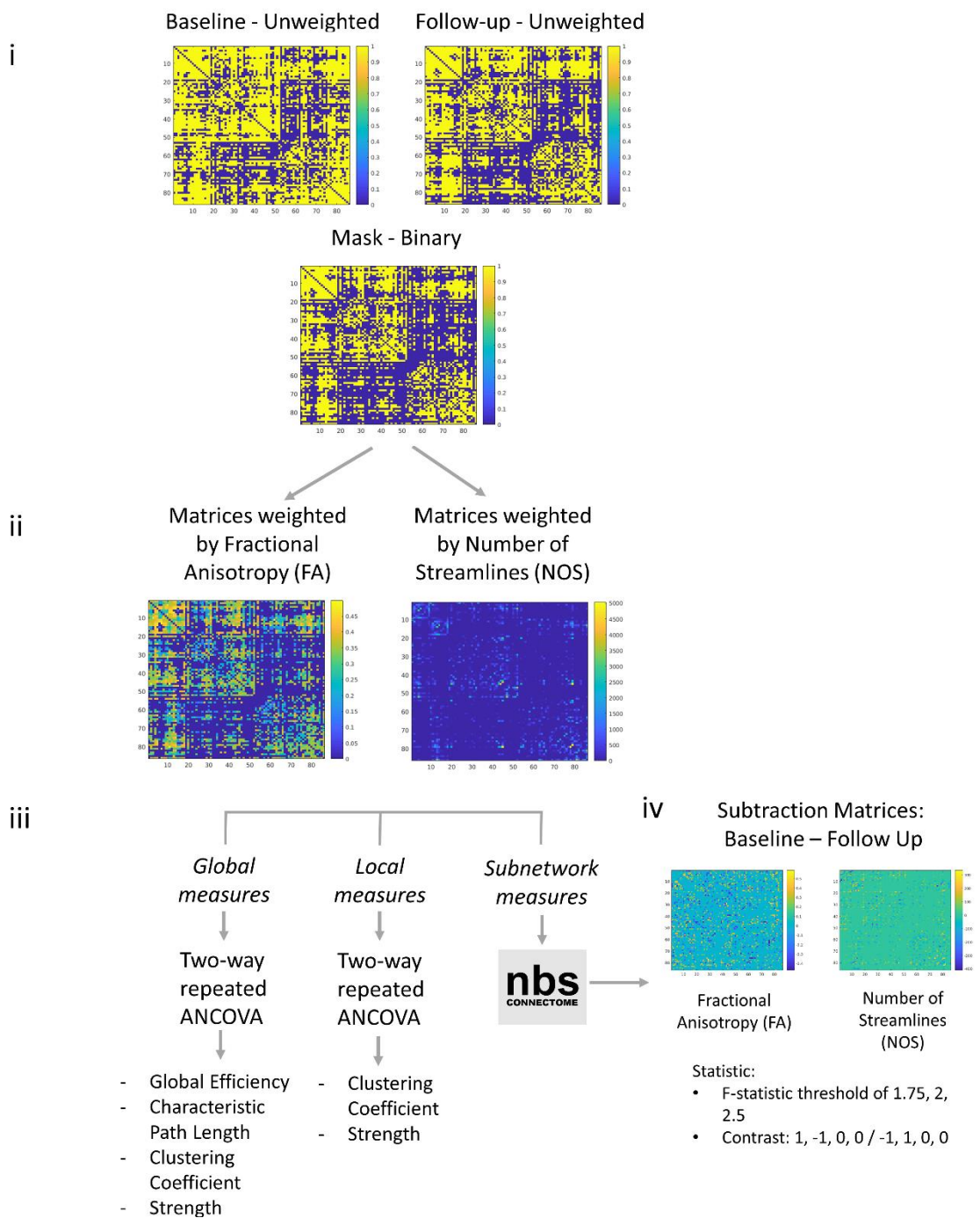- Contrast: 1, -1, 0, 0 / -1, 1, 0, 0

Figure 2. Network Reconstruction.

A) The image represents an overview of the steps to obtain structural connectivity matrices. Processing of T1-weighted images was performed through the longitudinal stream of Freesurfer v5.3.0 based on the Desikan-Killiany atlas (Desikan et al., 2006; Fischl., 2002) to parcellate 86 regions, including 34 cortical, 8 subcortical and cerebellar hemispheres bilaterally to create the nodes of the network. Processing of diffusion-weighted images was done using ExploreDTI v4.8.6, including motion correction, quality assessment and non-tensor-based constrained spherical deconvolution (CSD) tractography to obtain edges of the network (Jeurissen et al. 2011; Tournier et al. 2008). Unweighted and fractional anisotropy (FA)- and number of streamlines (NOS)-weighted structural matrices (86x86) were obtained for each participant and at each time point using ExploreDTI v4.8.6 by combining parcellated cortical and subcortical regions with CSD tractography-defined white matter. Fiber tracking commenced in each voxel, continued with 1 mm step size, 2 mm^3 seed point resolution, and terminated at >30° angle curvature, <20 or >300 mm in length, and <0.2 FA. B) The image represents the longitudinal design applied to the structural connectivity metrices. i) For each participant, a mask was created using unweighted connectivity matrices to include only the connections present at both baseline and follow-up. ii) The mask was used to threshold FA and NOS-weighted matrices. Quality check involved ensuring that post-thresholded networks remained fully connected which resulted in the removal of 1 healthy control iii) Global measures of whole-brain connectivity including global efficiency, characteristic path length, average clustering coefficient and average strength were derived from weighted matrices (Brain Connectivity Toolbox v1.52) (Rubinov and Sporns, 2010). Local measures of clustering coefficient and average strength were obtained for thalamus, putamen, caudate and hippocampus, whose volume was found decreased over time in patients compared to controls in our previous work (Tronchin et al., 2020a). Two-way repeated ANCOVA, covarying for age and sex was used for both local and global measures to assess differences over time on the connectivity measures between patients and controls. iv) We investigated the interaction between time and group on anatomical subnetwork connectivity using cluster-based statistical methods that control for the family-wise error rate (FWER) (network-based statistic, NBS v1.2). Using the thresholded matrices weighted by FA and NOS, we created a new matrix for the analysis, obtained by subtracting baseline from follow-up for each participant. A F-statistic representing the interaction between time and group for each connection was calculated using a general linear model (Pearson's correlation equivalent). A F-statistic threshold of 1.75, 2 and 2.5 corresponding to p<0.043, 0.02, 0.008 was applied and 5000 permutations used to calculate FWER-corrected p-values (pFWE) at 0.05 for every remaining connected component against a null distribution of maximum component size (Zalesky et al., 2010).

2.7 Anatomical Subnetwork Connectivity

We investigated the interaction between time and group on anatomical subnetwork connectivity using cluster-based statistical methods that control for the family-wise error rate (FWER) (network-based statistic, NBS v1.2). To do so, subtraction matrices were formed by subtracting the weighted and thresholded matrices at the follow-up from those at the baseline. A F-statistic representing the interaction between time and group for each connection was calculated using a general linear model (Pearson's correlation equivalent). A F-statistic threshold of 1.75, 2 and 2.5 corresponding to p<0.043, 0.02, 0.008 respectively was applied and 5000 permutations were used to calculate FWER-corrected p-values (pFWE) at 0.05 for every remaining connected component against a null distribution of maximum component size (Zalesky et al., 2010). A visual description of the methodological pipeline is outlined in Figure 2.

3. Results

3.1 Clinical characteristics

The patient and control groups did not differ in age, sex, or time between scans (Table 1). After treatment with clozapine, patients displayed a statistically significant improvement in PANSS, SANS, SAPS and GAF as previously reported (Ahmed et al., 2015; Tronchin et al., 2020a). At follow-up, patients also displayed a significant increase of weight, waist circumference, body mass index, and total cholesterol compared to baseline (Table 2). Ten patients were prescribed typical antipsychotic drugs at some stage of their illness and 2 were still taking first generation antipsychotic medications at the timepoint of the baseline scan. At baseline before switching to clozapine, 15 patients were on monotherapy with one second generation antipsychotic medication (olanzapine=5, quetiapine=1, aripiprazole=5, amisulpiride=1, paliperidone=1, risperidone long acting injection=1), 7 patients were treated with two antipsychotic medications (olanzapine + another antipsychotic=5), with one patient treated with four antipsychotic medications. At follow-up 11 patients (50%) had achieved remission.

Table 1. Characteristics of patients with treatment resistant-schizophrenia and controls

	Patient group (n=22)	Control group (n=23)	Test statistic/p-value
Sex (m/f)	16/6	14/9	X^2= 0.71; 0.399
Age at onset (years)	23.3 ± 4.9		
Age at baseline (years)	37.1 ± 9.5	41.3 ± 10.3	t= 1.43; 0.161
Age range	(22-51)	(23-55)	
Time between baseline and follow-up MRI scans (months)	6.5 ± 1.6	7.2 ± 1.8	t= 1.42; 0.163
Illness duration before commencing clozapine (years)	13.8 ± 7.9		

Table 2. Clinical features of patient group at baseline and follow-up (n=22)

	Baseline (Mean ± SD)	Follow-up (Mean ± SD)	Test statistic/ p-value
Clinical scales			
PANSS positive score	12.2 ± 5.1	5.8 ± 4.5	*z=-4.05; < 0.001
PANSS negative score	15.8 ± 7.2	9.0 ± 6.6	t=5.32; < 0.001
PANSS general score	21.5 ± 7.5	11.3 ± 8.1	t=7.77; < 0.001
PANSS total score	49.5 ± 16.7	26.1 ± 16.9	t=7.76; < 0.001
SANS	42.9 ± 20.6	28.9 ± 22.2	*z=-3.02; 0.003
SAPS	25.7 ± 10.2	13.2 ± 11.1	*z=-3.62; < 0.001
Global assessment of functioning	47.1 ± 9.5	63.9 ± 14.0	t = -5.15; < 0.001
Medications			
Typical antipsychotics (n)	3	0	
Atypical antipsychotics (n)	22	2	
Clozapine (n)	0	22	
Serum level of clozapine at follow-up (ng/ml)		0.4 ± 0.3	
Daily dose of clozapine at follow-up (mg)		336.4 ± 85.1	
Daily dose of clozapine range (mg)		(200-550)	
Anthropomorphic measurements			
Weight (kg)	85.0 ± 14.7	87.1 ± 15.0	t=-2.91; 0.008
Waist circumference (cm)	98.1 ± 13.0	103.3 ± 15.0	t=-4.22; <0.001
Body Mass Index	27.5 ± 5.1	28.2 ± 5.0	t=-2.90; 0.009
Total Cholesterol (mmol/L)	5.0 ± 0.8	5.5 ± 0.7	t=-2.16; 0.049
Triglycerides (mmol/L)	1.8 ± 1.2	2.0 ± 1.1	*z=-0.77; 0.443

Note: *= variable non-normal distributed; PANSS: Positive and negative Syndrome scale; SANS: The Scale for the Assessment of Negative Symptoms; SAPS: The Scale for the Assessment of Positive Symptoms. PANSS 0-6 scale was used. Ten patients were prescribed typical antipsychotic drugs at some stage of their illness
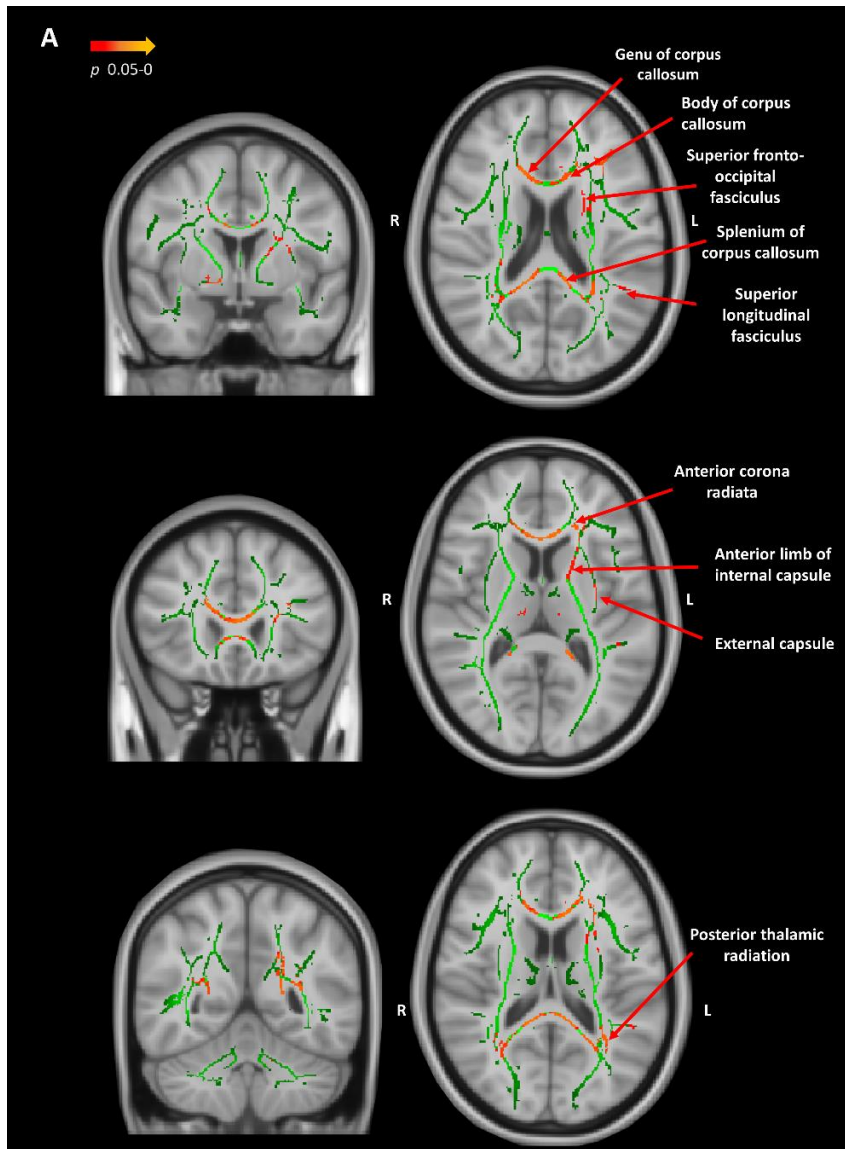
3.2 Voxel-based Statistical Analysis

      3.2.1 *Baseline comparison*

When investigating differences between groups at baseline, 7 significant clusters (Table 3) were found where the highest statistical group difference was identified using a p-value threshold of $p < 0.05$, showing lower FA in treatment-resistant schizophrenia patients compared to controls, consistent with the baseline comparison reported in a smaller sample (Holleran et al., 2013). The clusters included genu, body and splenium of the corpus callosum, bilaterally anterior, superior and posterior corona radiata, posterior thalamic radiation, external capsule, bilaterally anterior and posterior limb of intern capsule, right retrolenticular part of internal capsule, left superior longitudinal fasciculus, left superior fronto-occipital fasciculus, cingulum, bilaterally tapetum; fornix, bilaterally medial lemniscus, cerebellar peduncles and bilaterally cortico-spinal tract (Figure 3A). In terms of baseline neuroimaging metrics predicting clinical change, there was a significant moderate correlation between mean FA at baseline extracted from the largest cluster (Cluster n.7) in patients and change in SANS ($r = 0.532$, $p = 0.016$) (Figure 3B), but no significant correlations between mean FA at baseline and change in other clinical and anthropomorphic variables or serum level of clozapine at follow-up (Suppl. Table 1). When investigating the baseline differences between those who remitted on clozapine treatment (n=11) and non-responders (n=11) for the largest cluster (Cluster n.7), no significant differences were revealed ($F(1, 18 = 3.179$, $p = 0.091$.

Table 3. Significant white matter clusters of lower fractional anisotropy at baseline and reduce over time between patients and controls

CLUSTER INDEX	REGIONS	VOXELS	MAX	MAX x (vox)	MAX y (vox)	MAX z (vox)	COG x (vox)	COG y (vox)	COG z (vox)
Baseline									
7	- Genu, body, splenium of corpus callosum - Anterior, posterior, superior corona radiata R/L - Anterior limb of internal capsule L - Posterior thalamic radiation R/L - External capsule L - Cingulum (cingulate gyrus) L - Superior longitudinal fasciculus L - Superior fronto-occipital fasciculus L	7249	0.974	95	110	98	94.5	115	92.3
6	- Pontine crossing tract - Corticospinal tract R/L - Medial lemniscus R/L	2493	0.967	72	110	65	84.1	108	66.1
5	- Corticospinal tract R/L - Cerebral peduncle R/L - Anterior limb of internal capsule R - Posterior limb of internal capsule R/L - Retrolenticular part of internal capsule R - Fornix (cres) R	341	0.952	90	89	29	90.5	91.2	37.7
4	- Middle cerebellar peduncle	60	0.952	74	100	44	75.2	102	42.6
3	- Corticospinal tract L	24	0.951	94	100	37	94.9	102	38.1
2	- Superior longitudinal fasciculus	11	0.95	133	81	91	132	79.8	94.2
1	- Inferior cerebellar peduncle L	10	0.95	95	85	30	96.4	85.5	30.3
Over time									
1	- Genu and body of corpus callosum - Anterior and superior corona radiata R/L	1181	0.966	83	150	82	94.2	147	89.9

Note: Table reporting the different significant clusters, their size, and information about their location and contents. Cluster Index: a number for each cluster from 1 to N (larger clusters have bigger numbers); Regions: list of regions included in each cluster, identified using the John Hopkins University (JHU) ICBM_DTI_81 White-Matter Labels atlas (Wakana et al., 2007); Voxels: number of voxels in the cluster; MAX: the value of the z-statistic, 0.95 corresponds to a p-value of 0.05 ; MAX x/y/z: the location of the maximum intensity voxel, given as X/Y/Z coordinate values in voxel coordinates (vox); COG X/Y/Z (vox): the location of the Centre Of Gravity for the cluster ("fslwiki Cluster," 2013)
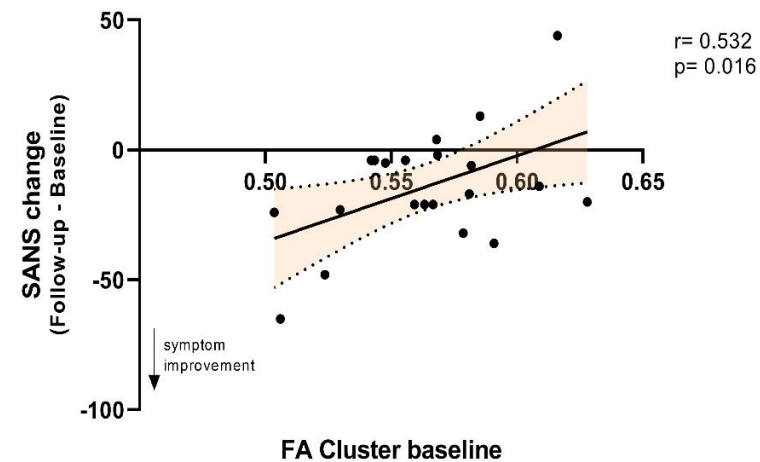
Figure 3. A) Fractional anisotropy (FA) differences at baseline between patients and controls. In the image the green represents the mean skeleton mask, in red (*p=0.05*) to yellow (lowest *p-value*) significant voxels for the biggest cluster (Cluster n.7) where FA was significantly lower in patients compared to controls (p<0.05, threshold-free cluster enhancement, TFCE). In red some of the main regions of lower FA (Fully listed in Table 3) in treatment-resistant schizophrenia patients compared to healthy controls: genu, body and splenium of corpus callosum, left superior longitudinal fasciculus, left superior fronto-occipital fasciculus, bilaterally anterior corona radiata, left interior limb of internal capsule, left external capsule and bilaterally posterior thalamic radiation. B) Correlation between FA at baseline (Cluster n.7) in patients and change in The Scale for the Assessment of Negative Symptoms (SANS). Negative values in SANS change reflect symptoms improvement over time.

3.2.2 *Longitudinal analysis*

When looking at differences in FA between treatment-resistant schizophrenia patients and controls over time, 1 significant cluster of voxels was found where the highest statistical group difference was identified using a p-value threshold of $p < 0.05$. The cluster showed greater change in FA in the patient group compared to controls over time, reflecting a FA reduction in the genu and body of the corpus callosum and bilaterally in the anterior corona radiata (ACR) and superior corona radiata (SCR) (Figures 4A,4B). There was no correlation between FA change in patients and any change in clinical and anthropomorphic variables or serum level of clozapine at follow-up (Suppl. Table 1). MD and RD were not significantly different between groups over time.

3.3 Network Connectivity

There was no significant difference between patients and controls at baseline ($F(8,33)= 1.66$; $p=0.146$, Table 4) when examining global measures of global efficiency, characteristic path length, clustering coefficient and strength weighted by FA and NOS and correcting for multiple comparisons. Likewise, when investigating the baseline differences between those who remitted on clozapine treatment (n=11) and non-responders (n=11) for global measures, no significant differences were found ($F8,11) = 2.123$, $p=0.123$).

There was no significant overall interaction between time, group and structural global measures ($F(7,280)=2.80$; $p= 0.187$, Table 4). Local measures of clustering coefficient and strength weighted by FA and NOS for thalamus, putamen, caudate and hippocampus (regions demonstrated in our previous study to reduce in volume over time (Tronchin et al., 2020a) did not show a significant overall difference between patients and controls at baseline ($F(15,26)=0.930$; $p=0.546$, Suppl. Table 2) or over time ($F(15,600)=0.747$, $p= 0.737$, Suppl. Table 2). The local measure of strength FA-weighted for caudate and weighted by NOS for thalamus showed a significant difference between patients and controls at the baseline and follow-up, although did not survive multiple comparison correction (Suppl. Table 2).

No subnetwork (weighted by FA and NOS) was identified when examining the time by group interaction.
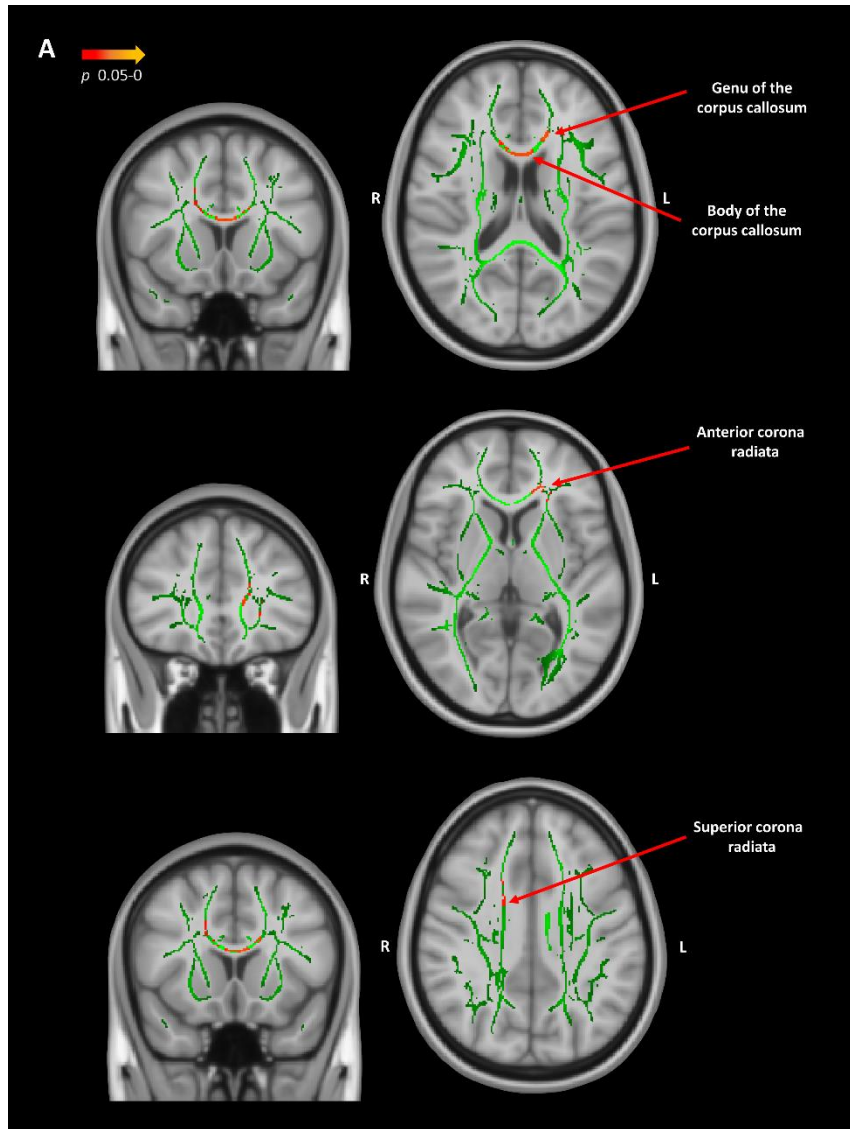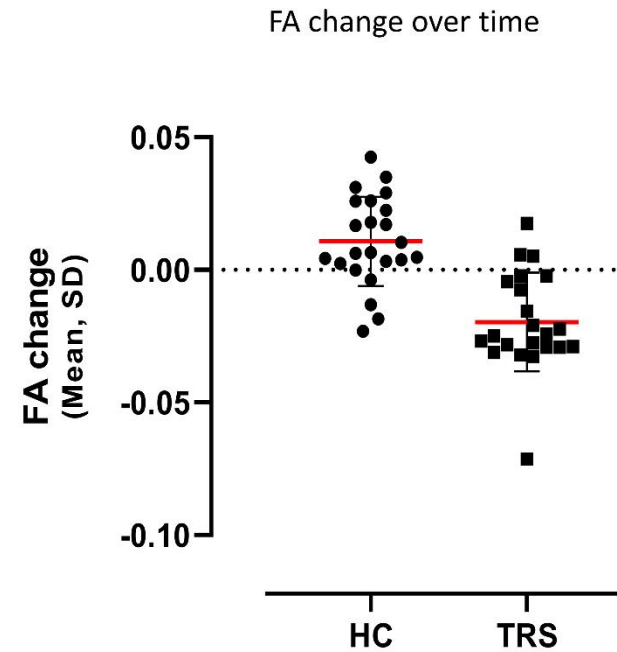
Figure 4. A) Fractional anisotropy (FA) differences over time between patients and controls. In the image the green represents the mean skeleton mask, in red (*p=0.05*) to yellow (lowest *p-value*) significant voxels where the change in FA from baseline to follow-up is significantly different between patients and controls (p< 0.05, threshold-free cluster enhancement, TFCE). In red regions of reduced FA over time in treatment-resistant schizophrenia patients compared to healthy controls in the body and genu of the corpus callosum, anterior corona radiata and bilaterally superior corona radiata. Radiological format is utilised.

B) Fractional anisotropy (FA) change over time. The graph represents the mean FA change from baseline to follow-up in the control and treatment-resistant schizophrenia groups within the significant cluster. The negative values reflect a reduction over time while positive values an increase.

Table 4. Uncorrected means (SD) for each global measure at baseline, follow-up, over time and results of statistical comparisons.

STRUCTURES	SCHIZOPHRENIA (n=22)	HEALTHY CONTROL (n =22)	GLM Baseline	SCHIZOPHRENIA (N=22)	HEALTHY CONTROL (N=22)	GLM Follow-Up	GLM Group*Time* Structure
	BASELINE	BASELINE	$F_{(8,33)}$ = 1.66, p= 0.146	FOLLOW-UP	FOLLOW-UP	$F_{(8,33)}$ = 1.32; p= 0.267	$F_{(7,280)}$ = 1.80; p=0.187
GLOBAL MEASURES			*p*			*p*	*p*
Global Efficiency	Means ± SD	Means ± SD		Means ± SD	Means ± SD		
FA	0.216 ± 0.013	0.220 ± 0.009	0.121	0.214 ± 0.014	0.218 ± 0.008	0.189	0.754
NOS	197.492 ± 25.403	213.240 ± 53.485	0.196	204.659 ± 41.149	195.907 ± 28.866	0.890	0.215
Characteristic Path Length							
FA	5.199 ± 0.330	5.072 ± 0.222	0.100	5.252 ± 0.384	5.131 ± 0.194	0.152	0.931
NOS	0.007 ± 0.002	0.007 ± 0.003	0.851	0.007 ± 0.002	0.007 ± 0.003	0.823	0.988
Global Clustering coefficient							
FA	0.5867 ± 0.030	0.594 ± 0.027	0.405	0.586 ± 0.029	0.592 ± 0.028	0.527	0.491
NOS	0.054 ± 0.011	0.050 ± 0.013	0.250	0.056 ± 0.010	0.048 ± 0.011	0.030	0.260
Global Strength							
FA	9.103 ±1.286	9.325 ± 1.110	0.509	9.004 ± 1.278	9.205 ± 1.120	0.562	0.786
NOS	4214.874 ± 700.274	4616.381 ± 1275.146	0.194	4363.440 ± 1060.191	4161.839 ± 709.172	0.858	0.187

Note: FA: fractional anisotropy; NOS: number of streamlines

4. *Discussion*

The longitudinal voxel-by-voxel based statistical analysis revealed a significant fractional anisotropy reduction over time in white matter microstructure in patients compared to controls, specifically in the genu and body of the corpus callosum and bilaterally in the anterior and superior corona radiata. Lower FA in the anterior corona radiata (Kelly et al., 2017) and body of the corpus callosum (Ellison-wright and Bullmore, 2009; Kelly et al., 2017; Vitolo et al., 2017) is the most prominent and reported finding from large cross-sectional studies and meta-analyses in schizophrenia and was again identified amongst the baseline group comparison findings in the current cohort. Our longitudinal findings suggest a progressive focal microstructural white matter abnormality in these critical regions in treatment-resistant schizophrenia patients.

4.1 Fractional anisotropy reduction

The progressive reduction of fractional anisotropy in the white matter of corpus callosum and corona radiata might be due to several factors. FA has been shown to be sensitive to the presence and microstructural organization of white matter fibers (Assaf and Pasternak, 2008). Change in this metric might be attributable for example to demyelination, oedema, inflammation or reduced axonal numbers. Anisotropy measures significantly change when myelin is damaged or when there is an elevated content of water in a tissue (Assaf and Pasternak, 2008; Beaulieu, 2002). Flynn and colleagues (2003) implementing MRI and T2 relaxation, which enables detection of signal related to water distribution in tissue (Whittall et al., 1997), showed reduced myelin water fraction in schizophrenia compared to healthy controls, with the left genu of the corpus callosum displaying the more prominent effect. The reduction was found to be greater in the chronic schizophrenia group compared to first-episode patients suggesting more pronounced abnormalities as the disease progresses (Flynn et al., 2003). A qualitative electron microscopy post-mortem study in patients with schizophrenia, reported signs of apoptosis and necrosis only in the oligodendroglia cells, which are responsible for the production of myelin sheath, that surrounds cell axons (Uranova et al., 2001). The fractional anisotropy reduction we observed in our study may reflect the impact of switching to clozapine on white matter (despite no association with serum level) or

may simply be completely independent of medication and related to the progression on white matter of the underlying pathophysiology of this malignant form of schizophrenia illness.

Corpus Callosum

The corpus callosum is the largest white matter interhemispheric pathway that links regions of the two hemispheres and is responsible for the integration and transfer of inter-hemispheric information to process sensory, motor, and high-level cognitive signals (Goldstein et al., 2020). Its disruption assumes an important role within the dysconnectivity hypothesis in schizophrenia (Friston and Frith, 1995) and is repeatedly reported in the literature using different methodological approaches (Pettersson-Yeo et al., 2011). Callosal white matter alteration has been proposed as a biomarker for chronic schizophrenia (Zhao et al., 2018). A recent cross-sectional DTI study reported low FA in white matter of body and splenium of the corpus callosum in treatment-resistant schizophrenia patients taking clozapine monotherapy compared to healthy controls (McNabb et al., 2019). In contrast to our study, a longitudinal DTI study by Ozcelik-Eroglu et al., (2014) based on 16 schizophrenia patients and 8 controls, reported in the patient group increased FA values in the corpus callosum at follow-up compared to baseline after 12 weeks of clozapine treatment (Ozcelik-Eroglu et al., 2014). There were several methodological differences between this and the current study which may account for these conflicting findings, including the statistical design implemented in the neuroimaging pipeline.

Corona Radiata

The corona radiata consists of a combination of association, projection and callosal fibers (Wakana et al., 2004) and interconnects the cerebral cortex with the thalamus and brainstem and is believed to be involved in information processing. Low FA values in anterior corona radiata have been associated with auditory verbal hallucination severity in schizophrenia (Ćurčić-Blake et al., 2013). McNabb and colleagues, investigating cross-sectional white matter aberrations in treatment-resistant subtypes of schizophrenia using DTI, reported low FA values in the superior and posterior corona radiata in patients on clozapine monotherapy compared to healthy controls (McNabb et al., 2019). Interestingly, consistent with our findings, a 6 weeks longitudinal study by Wang et al., (2013) on drug-naïve patients with schizophrenia reported a significant FA decrease in the white matter of the right corona

radiata in patients treated with antipsychotic medications compared to healthy controls (Wang et al., 2013).

In our previous work (Tronchin et al., 2020a) we found that progressive volumetric reduction of putamen and thalamus in patients after 6 months of clozapine treatment was significantly associated with symptom improvement, and patients who were exposed to higher amounts of clozapine displayed a greater reduction of thalamus volume. In this current study we did not find any correlation between FA reduction over time and change in clinical variables or serum level of clozapine at follow-up. Although the small sample size may have lacked statistical power to detect an association between FA change and clinical variables, any such association is likely to be very weak on the basis of the correlation coefficients detected, in contrast to the moderate associations detected for subcortical volume reduction that we reported in a similar sample (Tronchin et al., 2020a).

This result might suggest that in contrast to our previous study, the progressive fractional anisotropy reduction is not happening in the same individuals as the grey matter reduction and therefore not linked to symptomatic improvement, which could indicate an indiscriminate effect of switching to clozapine treatment without functional implications.

Consistent with this, longitudinal studies of first-episode antipsychotic drug-naive patients with schizophrenia reported FA change in the white matter of the corpus callosum and corona radiata which was not associated with symptom improvement or the dose of antipsychotic medication after 4 weeks or 6 weeks of antipsychotic treatment (Pan et al., 2016; Wang et al., 2013). While we found a reduction of FA over time in the patient group, we did not find a significant change over time between patient and controls in MD and RD. To the best of our knowledge there are no previous studies that have investigated longitudinal changes in MD or RD in schizophrenia patients.

At baseline, we found a widespread lower FA in the white matter of the patient group compared to healthy controls. The 7 significant clusters showed alteration in commissural and temporal lobe cortico-cortical fibres, confirming the findings reported in a previous work from our group on a smaller sample (Holleran et al., 2013). We found a significant correlation between lower FA values at baseline in the largest cluster in patients and improvement in negative symptoms over time. The lower the FA values in this cluster the greater the

improvement in negative symptoms over time in patients. The cluster included callosal, subcortical and fronto-temporal white matter regions. A similar counterintuitive relationship was reported in a longitudinal study by Molina and colleagues (2014) on first-episode schizophrenia, where the clinical improvement after 24 months of treatment was predicted by the baseline inferior frontal cortical thinning (Molina et al., 2014). Our finding warrants replication, but the lack of association between FA change in this region and negative symptom improvement indicates that any mechanism whereby clozapine improved negative symptoms in these patients is not mediated by change in this area.

4.2 Structural Network Connectivity

In our cohort, the structural network connectivity analysis found no difference between patients and controls at baseline or over time when examining global measures. We detected differences between patients and controls at baseline and follow-up on the local measure of strength weighted by FA for caudate and NOS for thalamus, however this did not survive multiple comparisons correction and requires investigation in a larger sample. We additionally did not find evidence that subnetwork connectivity changed differently over the 6-month period in patients compared to controls. A recent cross-sectional structural connectivity study did not find any difference between first episode schizophrenia and healthy controls on measures of clustering, path length or strength, while differences between chronic schizophrenia patients and healthy controls were found (Cea-Cañas et al., 2019). This suggests progression of dysconnectivity over time however the study lacks longitudinal arm. Our results are in contrast to several cross-sectional structural connectivity studies in chronic schizophrenia where altered global and local connectivity has been identified (Van Den Heuvel et al., 2010), as well as altered sub-networks compared to healthy controls (Collin et al., 2013; Zalesky et al., 2011). To date, there are no longitudinal studies that examine structural network connectivity over time in schizophrenia patients compared to healthy controls.

The preserved structural network findings in our study are in contrast to the focal areas of decreased fractional anisotropy at baseline and over time in this cohort of treatment-resistant schizophrenia patients. The lack of network level abnormalities suggests that despite evidence of focal progressive white matter microstructure abnormalities, the wider structural

brain network is not substantially impaired or significantly changed over a period of 6 months after commencement of clozapine treatment.

Strengths and Limitations

The main strength of the study is the longitudinal design combining different neuroimaging techniques to investigate the effect of 6 months of clozapine treatment on white matter microstructure and structural network organisation in a homogenous sample of treatment-resistant clozapine-naïve schizophrenia patients. The Freesurfer longitudinal pipeline used to define cortical and subcortical regions for the reconstruction of the structural network provided a subjects-specific parcellation (Desikan et al., 2006; Reuter et al., 2012; Reuter and Fischl, 2011) to increase the anatomical sensitivity. The reconstruction of estimated white matter trajectories was performed using a deterministic non-tensor-based constrained spherical deconvolution (CSD) algorithm, capable of deconvolving multiple fiber populations within a single voxel rather than the voxel-wise averages obtained using diffusion tensor tractography (Tournier et al., 2008).The CSD-deterministic approach has also been shown to have a lower number of false positives compared to CSD-probabilistic methods (Sarwar et al., 2019). A potential limitation of this study is the sample size, which may have provided limited sensitivity to detect more subtle effects. Additionally, our study did not have a comparative group of schizophrenia patients treated with other antipsychotic medications, in order to tease apart disease progression from treatment effects. However, this comparative group may represent a form of illness that is less malignant than treatment-resistant schizophrenia and subsequently show a different pattern of disease progression.

Conclusion

This longitudinal study demonstrated progressive fractional anisotropy abnormalities in the white matter microstructure of key anterior tracts, such as corpus callosum and corona radiata, and preserved brain structural network in a cohort of refractory schizophrenia. The FA reduction we observed was not associated with clinical improvement or clozapine serum level at follow-up, and may be associated with switching antipsychotic treatment to clozapine or with progression of the underlying pathophysiology of this malignant form of schizophrenia illness. Further longitudinal studies with larger sample size and randomised controlled designs will be necessary to better disentangle such disease related from medication related effects.

References:

Ahmed, M., Cannon, D.M., Scanlon, C., Holleran, L., Schmidt, H., McFarland, J., Langan, C.,
McCarthy, P., Barker, G.J., Hallahan, B., McDonald, C., 2015. Progressive Brain Atrophy
and Cortical Thinning in Schizophrenia after Commencing Clozapine Treatment.
Neuropsychopharmacology 40, 2409–2417. https://doi.org/10.1038/npp.2015.90

Anderson, V.M., Goldstein, M.E., Kydd, R.R., Russell, B.R., 2015. Extensive Gray Matter
Volume Reduction in Treatment-Resistant Schizophrenia. Int. J.
Neuropsychopharmacol. 1–10. https://doi.org/10.1093/ijnp/pyv016

Andreasen, N.C., 1982a. The scale for the assessment of Positive symptoms (SAPS). Iowa
City, Iowa Univ. Iowa.

Andreasen, N.C., 1982b. The Scale for the Assessment of Negative Symptoms (SANS). Iowa
City, Iowa Univ. Iowa.

Andreasen, N.C., Carpenter, W.T., Kane, J.M., Lasser, R.A., Marder, S.R., Weinberger, D.R.,
2005. Remission in Schizophrenia: Proposed Criteria and Rationale for Consensus. Am.
J. Psychiatry 162, 441–449. https://doi.org/10.1176/appi.ajp.162.3.441

Assaf, Y., Pasternak, O., 2008. Diffusion tensor imaging (DTI)-based white matter mapping in
brain research: A review. J. Mol. Neurosci. 34, 51–61. https://doi.org/10.1007/s12031-
007-0029-0

Beaulieu, C., 2002. The basis of anisotropic water diffusion in the nervous system - A
technical review. NMR Biomed. 15, 435–455. https://doi.org/10.1002/nbm.782

Bleuler, E., 1911. Dementia Praecox oder Gruppe der Schizophrenien. Leipzig, Ger. Deuticke.

Bora, E., Fornito, A., Radua, J., Walterfang, M., Seal, M., Wood, S.J., Yücel, M., Velakoulis, D.,
Pantelis, C., 2011. Neuroanatomical abnormalities in schizophrenia : A multimodal
voxelwise meta-analysis and meta-regression analysis. Schizophr. Res. 127, 46–57.
https://doi.org/10.1016/j.schres.2010.12.020

Cea-Cañas, B., de Luis, R., Lubeiro, A., Gomez-Pilar, J., Sotelo, E., del Valle, P., Gómez-García,
M., Alonso-Sánchez, A., Molina, V., 2019. Structural connectivity in schizophrenia and
bipolar disorder: Effects of chronicity and antipsychotic treatment. Prog. Neuro-
Psychopharmacology Biol. Psychiatry 92, 369–377.
https://doi.org/10.1016/j.pnpbp.2019.02.006

Chakos, M., Lieberman, J., Hoffman, E., Bradford, D., Sheitman, B., 2001. Effectiveness of

second-generation antipsychotics in patients with treatment-resistant schizophrenia: A review and meta-analysis of randomized trials. Am. J. Psychiatry 158, 518–526. https://doi.org/10.1176/appi.ajp.158.4.518

Collin, G., de Reus, M.A., Cahn, W., Hulshoff Pol, H.E., Kahn, R.S., van den Heuvel, M.P., 2013. Disturbed grey matter coupling in schizophrenia. Eur. Neuropsychopharmacol. 23, 46–54. https://doi.org/10.1016/j.euroneuro.2012.09.001

Ćurčić-Blake, B., Nanetti, L., van der Meer, L., Cerliani, L., Renken, R., Pijnenborg, G.H.M., Aleman, A., 2013. Not on speaking terms: hallucinations and structural network disconnectivity in schizophrenia. Brain Struct. Funct. 220, 407–418. https://doi.org/10.1007/s00429-013-0663-y

De Groot, M., Cremers, L.G.M., Arfan Ikram, M., Hofman, A., Krestin, G.P., Van Der Lugt, A., Niessen, W.J., Vernooij, M.W., 2016. White matter degeneration with aging: Longitudinal diffusion MR imaging analysis. Radiology 279, 532–541. https://doi.org/10.1148/radiol.2015150103

Desikan, R.S., Ségonne, F., Fischl, B., Quinn, B.T., Dickerson, B.C., Blacker, D., Buckner, R.L., Dale, A.M., Maguire, R.P., Hyman, B.T., Albert, M.S., Killiany, R.J., 2006. An automated labeling system for subdividing the human cerebral cortex on MRI scans into gyral based regions of interest. Neuroimage 31, 968–980. https://doi.org/10.1016/j.neuroimage.2006.01.021

Egerton, A., Broberg, B. V., Van Haren, N., Merritt, K., Barker, G.J., Lythgoe, D.J., Perez-Iglesias, R., Baandrup, L., Düring, S.W., Sendt, K. V., Stone, J.M., Rostrup, E., Sommer, I.E., Glenthøj, B., Kahn, R.S., Dazzan, P., McGuire, P., 2018. Response to initial antipsychotic treatment in first episode psychosis is related to anterior cingulate glutamate levels: a multicentre 1 H-MRS study (OPTiMiSE). Mol. Psychiatry 23, 2145–2155. https://doi.org/10.1038/s41380-018-0082-9

Ellison-wright, I., Bullmore, E., 2009. Meta-analysis of diffusion tensor imaging studies in schizophrenia. Schizophr. Res. 108, 3–10. https://doi.org/10.1016/j.schres.2008.11.021

Flynn, S.W., Lang, D.J., Mackay, A.L., Goghari, V., Vavasour, I.M., Whittall, K.P., Smith, G.N., Arango, V., Mann, J.J., Dwork, A.J., Falkai, P., Honer, W.G., 2003. Abnormalities of myelination in schizophrenia detected in vivo with MRI, and post-mortem with analysis of oligodendrocyte proteins. Mol. Psychiatry 8, 811–820. https://doi.org/10.1038/sj.mp.4001337

Fornito, A., Zalesky, A., Pantelis, C., Bullmore, E.T., 2012. Schizophrenia, neuroimaging and connectomics. Neuroimage 62, 2296–2314. https://doi.org/10.1016/j.neuroimage.2011.12.090

FreeSurfer [WWW Document], 2013. URL https://surfer.nmr.mgh.harvard.edu/ (accessed 10.2.18).

FreeSurfer Quality Control Guide [WWW Document], 2013. URL https://sites.bu.edu/cnrlab/lab-resources/freesurfer-quality-control-guide/ (accessed 10.2.18).

Friston, K.J., Frith, C.D., 1995. Schizophrenia: a disconnection syndrome? Clin. Neurosci. https://doi.org/10.1007/s00117-004-1160-3

FSL Support [WWW Document], n.d. URL https://www.jiscmail.ac.uk/cgi-bin/webadmin

fslwiki Cluster [WWW Document], 2013. URL https://fsl.fmrib.ox.ac.uk/fsl/fslwiki/Cluster

Ganella, E.P., Bartholomeusz, C.F., Seguin, C., Whittle, S., Bousman, C., 2017. Functional brain networks in treatment-resistant schizophrenia. Schizophr. Res. 184, 73–81. https://doi.org/10.1016/j.schres.2016.12.008

Goldstein, A., Covington, B.P., Mahabadi, N., Mesfin, F.B., 2020. Neuroanatomy, Corpus Callosum. Treasure Island (FL).

Hall, R.C.W., 1995. Global Assessment of Functioning: A Modified Scale. Psychosomatics 36, 267–275. https://doi.org/10.1016/S0033-3182(95)71666-8

Holleran, L., Ahmed, M., Anderson-schmidt, H., Mcfarland, J., Emsell, L., Leemans, A., Scanlon, C., Dockery, P., Mccarthy, P., Barker, G.J., Mcdonald, C., Cannon, D.M., 2013. Altered Interhemispheric and Temporal Lobe White Matter Microstructural Organization in Severe Chronic Schizophrenia 39, 944–954. https://doi.org/10.1038/npp.2013.294

Jones, D.K., 2008. Studying connections in the living human brain with diffusion MRI. Cortex 44, 936–952. https://doi.org/10.1016/j.cortex.2008.05.002

Kane, J., Honigfeld, G., Singer, J., Meltzer, H., 1988. Clozapine for the treatment-resistant schizophrenic. A double-blind comparison with chlorpromazine. Arch. Gen. Psychiatry 45, 789–796. https://doi.org/10.1001/archpsyc.1988.01800330013001

Kay, S.R., Fiszbein, A., Opler, L.A., 1987. The positive and negative syndrome scale (PANSS) for schizophrenia. Schizophr. Bull. 13, 261–276.

Kelly, S., Jahanshad, N., Zalesky, A., Kochunov, P., Agartz, I., Alloza, C., Andreassen, O.A.,

Arango, C., Banaj, N., Bouix, S., 2017. Widespread white matter microstructural differences in schizophrenia across 4322 individuals : results from the ENIGMA Schizophrenia DTI Working Group. Nat. Publ. Gr. 23, 1261–1269. https://doi.org/10.1038/mp.2017.170

Kraguljac, N.V., Anthony, T., Skidmore, F.M., Marstrander, J., Morgan, C.J., Reid, M.A., White, D.M., Jindal, R.D., Melas Skefos, N.H., Lahti, A.C., 2019. Micro- and Macrostructural White Matter Integrity in Never-Treated and Currently Unmedicated Patients With Schizophrenia and Effects of Short-Term Antipsychotic Treatment. Biol. Psychiatry Cogn. Neurosci. Neuroimaging 4, 462–471. https://doi.org/10.1016/j.bpsc.2019.01.002

Leemans, A., Jeurissen, B., Sijbers, J., Jones, D.K., 2009. ExploreDTI: a graphical toolbox for processing, analyzing, and visualizing diffusion MR data. Proc. Int. Soc. Magn. Reson. Med. 17, 3537.

Lieberman, J.A., Safferman, A.Z., Pollack, S., Szymanski, S., Johns, C., Howard, A., Kronig, M., Bookstein, P., Kane, J.M., 1994. Clinical effects of clozapine in chronic schizophrenia: response to treatment and predictors of outcome. Am. J. Psychiatry 151, 1744–1752. https://doi.org/10.1176/ajp.151.12.1744

Luo, C., Lencer, R., Hu, N., Xiao, Y., Zhang, W., Li, S., Lui, S., Gong, Q., 2020. Characteristics of White Matter Structural Networks in Chronic Schizophrenia Treated With Clozapine or Risperidone and Those Never Treated. Int. J. Neuropsychopharmacol. 23, 799–810. https://doi.org/10.1093/ijnp/pyaa061

Mackay, M.B., Paylor, J.W., Wong, J.T.F., Winship, I.R., Baker, G.B., Dursun, S.M., 2018. Multidimensional Connectomics and Treatment-Resistant Schizophrenia : Linking Phenotypic Circuits to Targeted Therapeutics 9. https://doi.org/10.3389/fpsyt.2018.00537

Maller, J.J., Daskalakis, Z.J., Thomson, R.H.S., Daigle, M., Barr, M.S., Fitzgerald, P.B., 2012. Hippocampal Volumetrics in Treatment-Resistant Depression and Schizophrenia : The Devil's in De-Tail. Hippocampus 22, 9–16. https://doi.org/10.1002/hipo.20873

McNabb, C.B., McIlwain, M.E., Anderson, V.M., Kydd, R., Sundram, F., Russell, B.R., 2019. Disrupted white matter integrity in treatment-resistant schizophrenia. https://doi.org/10.1101/19010777

Meltzer, H.Y., 1997. Treatment-resistant schizophrenia--the role of clozapine. Curr. Med.

Res. Opin. 14, 1–20. https://doi.org/10.1185/03007999709113338

Minett, T., Su, L., Mak, E., Williams, G., Firbank, M., Lawson, R.A., Yarnall, A.J., Duncan, G.W., Owen, A.M., Khoo, T.K., Brooks, D.J., Rowe, J.B., Barker, R.A., Burn, D., O'Brien, J.T., 2018. Longitudinal diffusion tensor imaging changes in early Parkinson's disease: ICICLE-PD study. J. Neurol. 265, 1528–1539. https://doi.org/10.1007/s00415-018-8873-0

Molina, V., Reig, S., Sanz, J., Palomo, T., Benito, C., Sarramea, F., Pascau, J., Sanchez, J., Martin-Loeches, M., Munoz, F., Desco, M., 2008. Differential clinical, structural and P300 parameters in schizophrenia patients resistant to conventional neuroleptics. Prog. Neuropsychopharmacol. Biol. Psychiatry 32, 257–266. https://doi.org/10.1016/j.pnpbp.2007.08.017

National Institute of Health and Clinical Excellence, 2014. Psychosis and schizophrenia in adults. NICE Guidel. treament Manag. 74–80. https://doi.org/10.1002/14651858.CD010823.pub2.Copyright

Nichols, T., Holmes, A., 2003. Nonparametric Permutation Tests for Functional Neuroimaging. Hum. Brain Funct. Second Ed. 25, 887–910. https://doi.org/10.1016/B978-012264841-0/50048-2

Ottet, M.C., Schaer, M., Debbané, M., Cammoun, L., Thiran, J.P., Eliez, S., 2012. Graph theory reveals dysconnected hubs in 22q11DS and altered nodal efficiency in patients with hallucinations. Front. Hum. Neurosci. 7. https://doi.org/10.3389/fnhum.2013.00402

Ozcelik-Eroglu, E., Ertugrul, A., Oguz, K.K., Has, A.C., Karahan, S., Yazici, M.K., 2014. Effect of clozapine on white matter integrity in patients with schizophrenia: A diffusion tensor imaging study. Psychiatry Res. - Neuroimaging 223, 226–235. https://doi.org/10.1016/j.pscychresns.2014.06.001

Pan, E., Ates, M.A., Algul, A., Aytekin, A., Basoglu, C., Ebrinc, S., Cetin, M., Kose, S., 2016. Fractional anisotropic changes of corpus callosum associated with antipsychotic treatment in first-episode antipsychotic drug-naive patients with schizophrenia. Klin. Psikofarmakol. Bul. 26, 332–341. https://doi.org/10.5455/bcp.20160319021659

Pettersson-Yeo, W., Allen, P., Benetti, S., McGuire, P., Mechelli, A., 2011. Dysconnectivity in schizophrenia: Where are we now? Neurosci. Biobehav. Rev. 35, 1110–1124. https://doi.org/10.1016/j.neubiorev.2010.11.004

Pierpaoli, C., Jezzard, P., Basser, P.J., Barnett, A., Di Chiro, G., 1996. Diffusion tensor MR imaging of the human brain. Radiology 201, 637–648. https://doi.org/10.1148/radiology.201.3.8939209

Reis Marques, T., Taylor, H., Chaddock, C., Dell'Acqua, F., Handley, R., Reinders, A.A.T.S., Mondelli, V., Bonaccorso, S., Diforti, M., Simmons, A., David, A.S., Murray, R.M., Pariante, C.M., Kapur, S., Dazzan, P., 2014. White matter integrity as a predictor of response to treatment in first episode psychosis. Brain 137, 172–182. https://doi.org/10.1093/brain/awt310

Reuter, M., Fischl, B., 2011. Avoiding asymmetry-induced bias in longitudinal image processing. Neuroimage 57, 19–21. https://doi.org/10.1016/j.neuroimage.2011.02.076

Reuter, M., Schmansky, N.J., Rosas, H.D., Fischl, B., 2012. Within-subject template estimation for unbiased longitudinal image analysis. Neuroimage 61, 1402–1418. https://doi.org/10.1016/j.neuroimage.2012.02.084

Rubinov, M., Sporns, O., 2010. Complex network measures of brain connectivity: Uses and interpretations. Neuroimage 52, 1059–1069. https://doi.org/10.1016/j.neuroimage.2009.10.003

Sarwar, T., Ramamohanarao, K., Zalesky, A., 2019. Mapping connectomes with diffusion MRI: deterministic or probabilistic tractography? Magn. Reson. Med. 81, 1368–1384. https://doi.org/10.1002/mrm.27471

Smith, S.M., Nichols, T.E., 2009. Threshold-free cluster enhancement: Addressing problems of smoothing, threshold dependence and localisation in cluster inference. Neuroimage 44, 83–98. https://doi.org/10.1016/j.neuroimage.2008.03.061

Song, S.K., Sun, S.W., Ju, W.K., Lin, S.J., Cross, A.H., Neufeld, A.H., 2003. Diffusion tensor imaging detects and differentiates axon and myelin degeneration in mouse optic nerve after retinal ischemia. Neuroimage 20, 1714–1722. https://doi.org/10.1016/j.neuroimage.2003.07.005

Song, S.K., Sun, S.W., Ramsbottom, M.J., Chang, C., Russell, J., Cross, A.H., 2002. Dysmyelination revealed through MRI as increased radial (but unchanged axial) diffusion of water. Neuroimage 17, 1429–1436. https://doi.org/10.1006/nimg.2002.1267

Stroup, T.S., Mcevoy, J.P., Swartz, M.S., Byerly, M.J., Qlick, I.D., Canive, J.M., Mcqee, M.F., Simpson, Q.M., Stevens, M.C., Lieberman, J.A., 2003. The National Institute of Mental

Health Clinical Antipsychotic Trials of Intervention Effectiveness (CATIE) Project : Schizophrenia Trial Design and Protocol Development. Schizophr. Bull.

Suzuki, T., Remington, G., Mulsant, B.H., Uchida, H., Rajji, T.K., Graff-guerrero, A., Mimura, M., Mamo, D.C., 2012. Defining treatment-resistant schizophrenia and response to antipsychotics : A review and recommendation. Psychiatry Res. 197, 1–6. https://doi.org/10.1016/j.psychres.2012.02.013

Tournier, J.-D., Mori, S., Leemans, A., 2011. Diffusion tensor imaging and beyond. Magn. Reson. Med. 65, 1532–1556. https://doi.org/10.1002/mrm.22924

Tournier, J.D., Yeh, C.H., Calamante, F., Cho, K.H., Connelly, A., Lin, C.P., 2008. Resolving crossing fibres using constrained spherical deconvolution: Validation using diffusion-weighted imaging phantom data. Neuroimage 42, 617–625. https://doi.org/10.1016/j.neuroimage.2008.05.002

Tronchin, G., Akudjedu, T.N., Ahmed, M., Holleran, L., Hallahan, B., Cannon, D.M., McDonald, C., 2020a. Progressive subcortical volume loss in treatment-resistant schizophrenia patients after commencing clozapine treatment. Neuropsychopharmacology 45, 1353–1361. https://doi.org/10.1038/s41386-020-0665-4

Tronchin, G., Akudjedu, T.N., Kenney, J.P., McInerney, S., Scanlon, C., McFarland, J., McCarthy, P., Cannon, D.M., Hallahan, B., McDonald, C., 2020b. Cognitive and Clinical Predictors of Prefrontal Cortical Thickness Change Following First-Episode of Psychosis. Psychiatry Res. Neuroimaging 302, 111100. https://doi.org/10.1016/j.pscychresns.2020.111100

Uranova, N., Orlovskaya, D., Vikhreva, O., Zimina, I., Kolomeets, N., Vostrikov, V., Rachmanova, V., 2001. Electron microscopy of oligodendroglia in severe mental illness. Brain Res. Bull. 55, 597–610. https://doi.org/10.1016/S0361-9230(01)00528-7

Van Den Heuvel, M.P., Fornito, A., 2014. Brain networks in schizophrenia. Neuropsychol. Rev. 24, 32–48. https://doi.org/10.1007/s11065-014-9248-7

Van Den Heuvel, M.P., Mandl, R.C.W., Stam, C.J., Kahn, R.S., Hulshoff Pol, H.E., 2010. Aberrant frontal and temporal complex network structure in schizophrenia: A graph theoretical analysis. J. Neurosci. 30, 15915–15926. https://doi.org/10.1523/JNEUROSCI.2874-10.2010

Vitolo, E., Tatu, M.K., Pignolo, C., Cauda, F., Costa, T., Ando, A., Zennaro, A., 2017. White

matter and schizophrenia: A meta-analysis of voxel-based morphometry and diffusion tensor imaging studies. Psychiatry Res. - Neuroimaging 270, 8–21. https://doi.org/10.1016/j.pscychresns.2017.09.014

Wakana, S., Caprihan, A., Panzenboeck, M.M., Fallon, J.H., Perry, M., Gollub, R.L., Hua, K., Zhang, J., Jiang, H., Dubey, P., Blitz, A., van Zijl, P., Mori, S., 2007. Reproducibility of quantitative tractography methods applied to cerebral white matter. Neuroimage 36, 630–644. https://doi.org/10.1016/j.neuroimage.2007.02.049

Wakana, S., Jiang, H., Nagae-Poetscher, L.M., Van Zijl, P.C.M., Mori, S., 2004. Fiber Tract-based Atlas of Human White Matter Anatomy. Radiology 230, 77–87. https://doi.org/10.1148/radiol.2301021640

Wang, Q., Cheung, C., Deng, W., Li, M., Huang, C., Ma, X., Wang, Y., Jiang, L., Sham, P.C., Collier, D.A., Gong, Q., Chua, S.E., McAlonan, G.M., Li, T., 2013. White-matter microstructure in previously drug-naive patients with schizophrenia after 6 weeks of treatment. Psychol. Med. 43, 2301–2309. https://doi.org/10.1017/S0033291713000238

Whittall, K.P., MacKay, A.L., Graeb, D.A., Nugent, R.A., Li, D.K.B., Paty, D.W., 1997. In vivo measurement of T2 distributions and water contents in normal human brain. Magn. Reson. Med. 37, 34–43. https://doi.org/10.1002/mrm.1910370107

Zalesky, A., Fornito, A., Bullmore, E.T., 2010. Network-based statistic: Identifying differences in brain networks. Neuroimage 53, 1197–1207. https://doi.org/10.1016/j.neuroimage.2010.06.041

Zalesky, A., Fornito, A., Seal, M.L., Cocchi, L., Westin, C.F., Bullmore, E.T., Egan, G.F., Pantelis, C., 2011. Disrupted axonal fiber connectivity in schizophrenia. Biol. Psychiatry 69, 80–89. https://doi.org/10.1016/j.biopsych.2010.08.022

Zhang, Y., Lin, L., Lin, C.P., Zhou, Y., Chou, K.H., Lo, C.Y., Su, T.P., Jiang, T., 2012. Abnormal topological organization of structural brain networks in schizophrenia. Schizophr. Res. 141, 109–118. https://doi.org/10.1016/j.schres.2012.08.021

Zhao, W., Guo, S., He, N., Yang, A.C., Lin, C.P., Tsai, S.J., 2018. Callosal and subcortical white matter alterations in schizophrenia: A diffusion tensor imaging study at multiple levels. NeuroImage Clin. 20, 594–602. https://doi.org/10.1016/j.nicl.2018.08.027

Supplementary Data.

Supplementary Table 1. Correlations between FA change and change in clinical variables in patients

	PANSS Total (Change)		SAPS (Change)		SANS (Change)		GAF (Change)		BMI (Change)		Total Cholesterol (Change)		Serum level of clozapine		Duration of illness	
CLUSTER n.7	r	p	r	p	r	p	r	p	r	P	r	P	r	p	r	p
FA baseline	0.29	0.214	0.39	0.086	0.53	0.016	-0.21	0.371	-0.13	0.658	-0.05	0.857	0.051	0.829	-0.12	0.628
CLUSTER n.1	r_s	p	r_s	p	r_s	p	r_s	p	r_s	p	r_s	p	r_s	p	r_s	p
FA change	0.13	0.557	-0.13	0.573	-0.01	0.976	0.04	0.846	-0.03	0.891	-0.16	0.548	-0.23	0.312	-0.17	0.439

Note: PANSS: Positive and Negative Syndrome Scale; SANS: The Scale for the Assessment of Negative Symptoms; SAPS: The Scale for the Assessment of Positive Symptoms.

Supplementary Table 2. Uncorrected means (SD) for each local measure at baseline, follow-up, over time and results of statistical comparisons.

STRUCTURES	SCHIZOPHRENIA (n=22)	HEALTHY CONTROL (n =22)	GLM Baseline	SCHIZOPHRENIA (N=22)	HEALTHY CONTROL (N=22)	GLM Follow-up	GLM Group*Time* Structure
	BASELINE	BASELINE	F (15,26) = 0.930, p= 0.546	FOLLOW-UP	FOLLOW-UP	F (16,25) = 1.45, p= 0.195	F (15,600) = 0.747 p= 0.737
LOCAL MEASURES	Means ± SD	Means ± SD		Means ± SD	Means ± SD		*p*
Clustering coefficient FA							
Thalamus	0.998 ± 0.059	1.001 ± 0.088	0.983	0.996 ± 0.0625	0.999 ± 0.0913	0.951	0.790
Caudate	1.120 ± 0.070	1.115 ± 0.089	0.796	1.116 ± 0.069	1.112 ± 0.092	0.852	0.705
Putamen	0.946 ± 0.087	0.969 ± 0.094	0.418	0.946 ± 0.088	0.969 ± 0.094	0.437	0.778
Hippocampus	1.101 ± 0.090	1.119 ± 0.093	0.463	1.098 ± 0.091	1.117 ± 0.100	0.491	0.949
Clustering coefficient NOS							
Thalamus	0.091 ± 0.017	0.090 ± 0.025	0.756	0.094 ± 0.017	0.084 ± 0.017	0.062	0.124
Caudate	0.084 ± 0.016	0.089 ± 0.038	0.665	0.082 ± 0.015	0.075 ± 0.015	0.113	0.211
Putamen	0.096 ± 0.019	0.092 ± 0.030	0.670	0.100 ± 0.019	0.086 ± 0.027	0.079	0.086
Hippocampus	0.087 ± 0.017	0.085 ± 0.026	0.718	0.092 ± 0.020	0.082 ± 0.021	0.132	0.203
Strength FA							
Thalamus	32.869 ± 4.337	33.518 ± 4.514	0.567	32.629 ± 4.355	33.136 ± 4.080	0.595	0.807
Caudate	23.278 ± 3.138	26.714 ± 5.413	**0.013**	22.590 ± 2.883	26.231 ± 5.029	**0.005**	0.620
Putamen	37.755 ± 4.365	36.948 ± 5.798	0.803	37.555 ± 4.6139	36.967 ± 5.797	0.889	0.635
Hippocampus	24.978 ± 3.696	27.029 ± 5.218	0.202	24.585 ± 3.486	26.555 ± 5.153	0.184	0.941
Strength NOS							
Thalamus	18915.272 ± 2920.514	23586.864 ± 7774.532	**0.008**	18478.000 ± 2631.897	21362.136 ± 5992.642	**0.010**	0.343
Caudate	7459.272 ± 1324.049	11873.409 ± 8912.924	0.051	7183.455 ± 2108.761	9096.364 ± 4432.507	0.055	0.329
Putamen	19959.591 ± 3218.098	21333.727 ± 11084.638	0.537	20383.182 ± 3891.720	17864.227 ± 5240.139	0.249	0.193
Hippocampus	27418.864 ± 4247.196	33207.136 ± 17872.649	0.183	9711.727 ± 1784.240	11982.364 ± 8031.365	0.199	0.490

Note: FA: fractional anisotropy; NOS: number of streamlines